

Magnetic circular dichroism of impurities in solids: MgO:Co

A. J. Mann and P. J. Stephens*

Department of Chemistry, University of Southern California, Los Angeles, California, 90007

(Received 9 April 1973)

The magnetic circular dichroism of a dilute MgO:Co single crystal in the visible-uv spectral region is reported. Several new $d \rightarrow d$ transitions, previously undetected and unobservable in the absorption spectrum, are identified. All bands exhibit complex fine structure, almost none of which is interpretable in terms of simple models for vibration-induced transitions of impurities in MgO.

I. INTRODUCTION

We present a study of the magnetic circular dichroism (MCD) and absorption spectra of a dilute MgO:Co²⁺ crystal. Our goals are twofold. First, we hope to extend the characterization of the octahedrally coordinated Co²⁺ ion in a simple, highly symmetrical environment. Studies of transition-metal ions in such systems, particularly in MgO and KMgF₃, have been¹ and remain of central importance in advancing fundamental understanding of the d -electron states of transition-metal ions. Second, we wish to display the advantages of MCD as a tool in the study of impurities in solids. Despite recent work by chemists and physicists,² the power of dichroism techniques, particularly in transition-metal spectroscopy, remains insufficiently appreciated.

This study follows earlier work on MgO:Ni²⁺³ and is limited to the visible-uv spectral region. MCD studies in the near infrared (ir) are in progress and preliminary reports have been published.^{4,5} A full account of these, and of investigations of KMgF₃:Co²⁺ and KMgF₃:Ni²⁺, will be reported in future publications.

II. EXPERIMENTAL

Absorption spectra and MCD were measured between 4 and 300 °K with a Cary 14 and a Cary 61 as described in previous publications.^{3,6} Early MCD experiments were carried out at Cary Instruments,⁷ with the collaboration of Duffield and Abu-Shumays. Subsequently, MCD data were obtained on identical equipment in our own laboratory. Absorption spectra at temperatures between 300 and 469 °K were obtained by heating the crystal.

Light was passed through (001) faces 2.6-mm apart of the MgO:Co crystal. The crystal was not high in optical quality: sections were cloudy and appreciable depolarization occurred when placed between crossed polarizers. However, the crystal produced negligible change in the circular dichroism (CD) of solutions containing *D*-*ddd*-cobalt tris-propylene diamine chloride, copper-*L*-proline, or nickel *d*-tartrate complexes when placed before the solutions and the effects of crystal imperfection on

the MCD data can be ignored.

Absorption and MCD data are illustrated in Figs. 1–14 and tabulated in Table I. A and $\Delta A = A_L - A_R$ are absorbance and CD, respectively. Positive magnetic (H) fields are parallel to the light propagation direction. Zeroth moments are defined by

$$\begin{aligned} \langle A \rangle_0 &= \int (A/\nu) d\nu, \\ \langle \Delta A \rangle_0 &= \int (\Delta A/\nu) d\nu. \end{aligned} \quad (1)$$

Original traces are shown for the weak bands to show the quality of the data and to avoid the (sometimes difficult) subtraction of baselines. MCD spectra at different temperatures are displaced in Figs. 6, 8, 9, 11, and 12 for the sake of clarity. In Fig. 4, the smooth sloping background (seen in Fig. 2) has been subtracted by fitting to a double-Gaussian dispersion. The MCD in Fig. 5 is plotted after subtraction of a flat baseline and the 17 000-cm⁻¹ band and normalization to $H = +10$ kG, assuming linearity with H (see Sec. III). In addition to the absorption spectra shown, the 23 000-cm⁻¹ band is clearly observed with a signal-to-noise ratio somewhat greater than unity. The dependence of spectra on instrumental bandwidth was checked wherever possible and no evidence of instrumental broadening was found at the bandwidths employed. Absolute wavelength accuracy varies between 0.4 and 1.0 nm.

Absorption spectra at liquid-helium temperatures have been reported previously for MgO:Co crystals.^{8,9} Our near-ir spectrum (Fig. 1) is very similar to that of Ralph and Townsend.⁹ The spectra both in this region and in the visible uv (Fig. 2) are somewhat more detailed than those of Pappalardo, Wood, and Linares,⁸ particularly for the 17 000- and 25 000-cm⁻¹ bands (Figs. 7 and 10). Where comparison is possible frequencies are in essential agreement. Low¹⁰ reported spectra at 77 °K and room temperature and found weak bands at 13 750, 14 200, 17 200, 24 600, and 28 500 cm⁻¹, in addition to the strong 9000- and 20 000-cm⁻¹ bands. We find no evidence of the 13 750-, 14 200-, or 28 500-cm⁻¹ bands and these are probably due to either impurities or ion aggregates.

The Co concentration is not known exactly. By

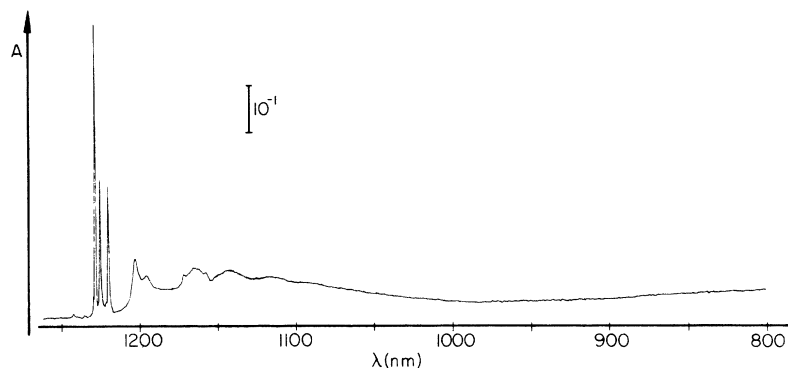


FIG. 1. Near-infrared absorption spectrum of $\text{MgO}:\text{Co}^{2+}$ at 7°K .

comparison with absorption spectra reported previously for crystals of known concentration,^{8,11} we estimate the Co-to-Mg ratio is approximately 2.6×10^{-3} . With this value we have

$$\epsilon = 16.9A, \quad (2)$$

$$f \approx (7.3 \times 10^{-8})\nu^0 \langle A \rangle_0,$$

where ϵ is the molar extinction coefficient and f and ν^0 are the oscillator strength and average frequency in cm^{-1} of a band.

The EPR spectrum of another crystal of the same origin was examined down to 4°K by Hurrell and showed the presence of small amounts of at least Cr^{3+} , Mn^{2+} , and Fe^{3+} . In addition, considerable weak fine structure was observed on and around the Co^{2+} spectrum, presumably due to perturbed Co^{2+} ions.

III. DISCUSSION

We wish to identify the bands observed in the absorption and MCD spectra with $d-d$ transitions of single Co^{2+} ions at O_h sites in the MgO lattice. Ligand-field theory¹² with reasonable parameters predicts states at energies in good agreement with those observed, as shown in Fig. 3 and Table I.¹³ The ground state of Co^{2+} is a Kramers doublet with $g = 4.278$.¹⁰ The MCD for such transitions would

then be expected to be dominated by C terms¹⁴ arising from the differential population of the ground-state Zeeman components, especially at low T , and should increase as T decreases. This is the case for the principal features of all bands, as shown by Figs. 5, 6, 8, 9, 11, and 12.¹⁵

The observation of more bands in MCD than in absorption (and the greater signal-to-noise ratio of those observed) arises from the high degree of circular polarization of the transitions and the relative sensitivities of the Cary 14 and Cary 61 instruments. For the 4T_1 band $\Delta A/A \sim 0.16$ at 12°K and 46 kG .¹⁶ With this circular polarization and a ΔA sensitivity $\sim 3 \times 10^{-6}$,¹⁷ bands with $A \gtrsim 2 \times 10^{-5}$ can be detected, as compared with $A \gtrsim 2 \times 10^{-3}$ by direct absorption measurement.

Estimates of the intensities of the transitions seen in MCD but not in absorption are given in Table I. These were obtained by assuming the ratio

$$\langle |\Delta A| \rangle_0 / \langle A \rangle_0,$$

(where

$$\langle |\Delta A| \rangle_0 = \int |\Delta A| / \nu d\nu)$$

to be the same for all bands, at the same H and T , and using the known $\langle A \rangle_0$ for the 4T_1 band.¹⁸ $\langle |\Delta A| \rangle_0$ is used instead of $\langle \Delta A \rangle_0$ since the MCD

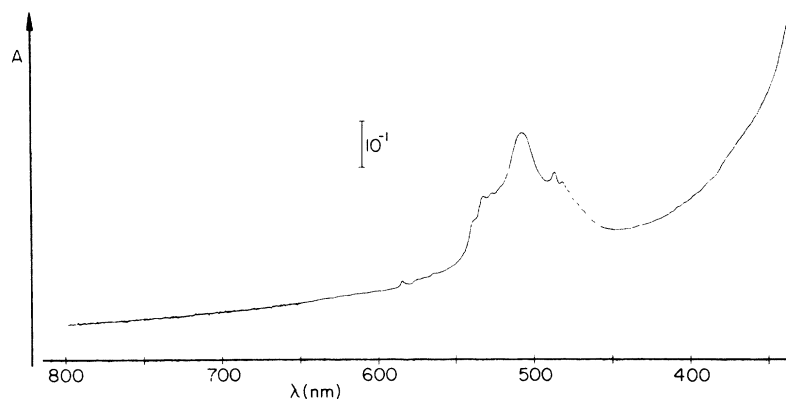


FIG. 2. Visible-near uv absorption spectrum of $\text{MgO}:\text{Co}^{2+}$ at 7°K .

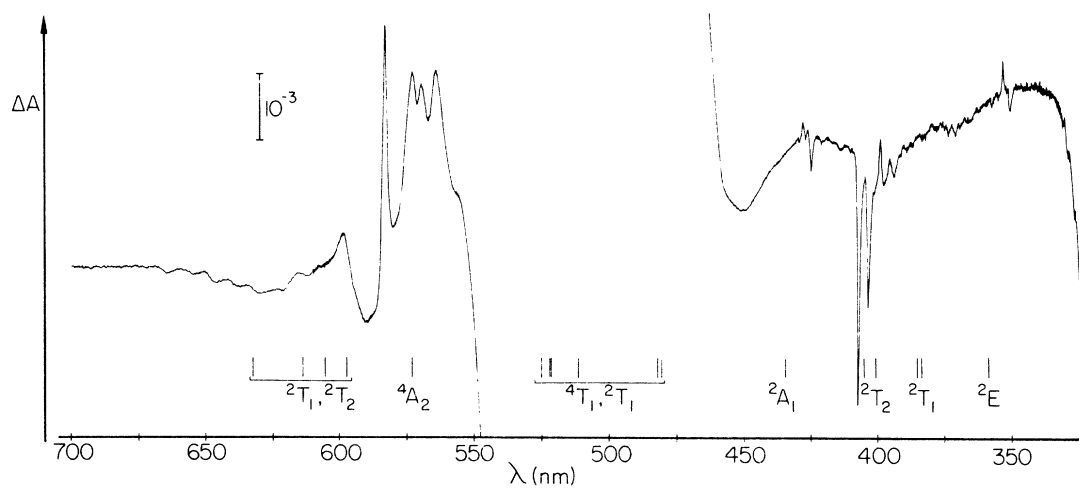


FIG. 3. Visible-near uv MCD spectrum of $\text{MgO}:\text{Co}^{2+}$ at 14°K , $H = +45.6 \text{ kG}$. Period 10 sec; spectral bandwidths 1 and 0.2 nm for $\lambda > 610 \text{ nm}$ and $\lambda < 610 \text{ nm}$, respectively.

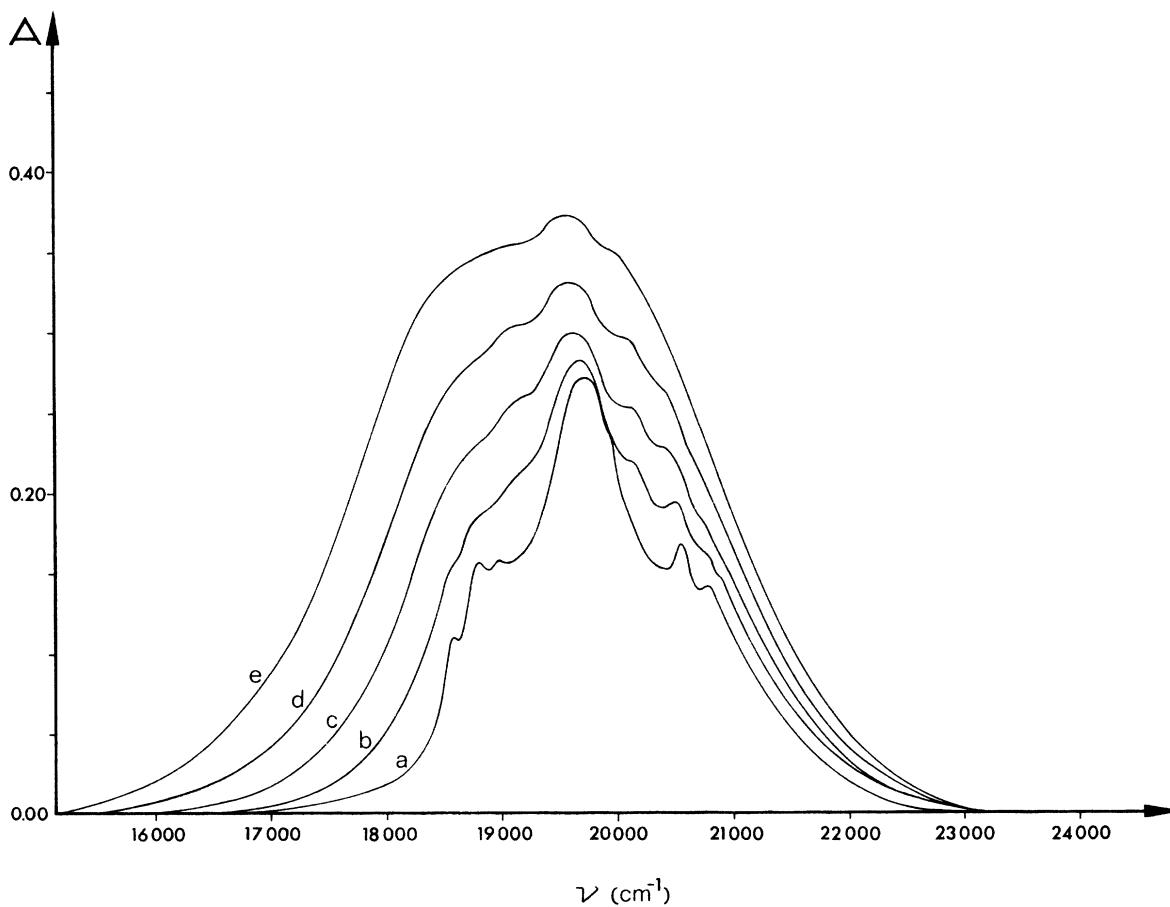


FIG. 4. Absorption spectrum of the $20\,000\text{-cm}^{-1}$ band of $\text{MgO}:\text{Co}^{2+}$ as a function of temperature: (a) 7°K , (b) 185°K , (c) 267°K , (d) 345°K , and (e) 469°K . Curved baselines and the weak band at $17\,000 \text{ cm}^{-1}$ have been subtracted. Spectral bandwidth $\sim 0.23 \text{ nm}$.

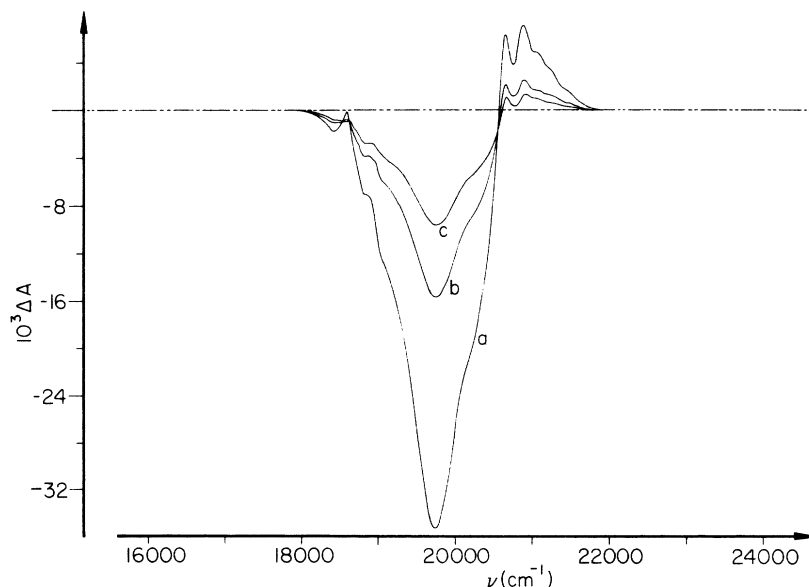


FIG. 5. MCD spectrum of the 20 000-cm⁻¹ band of MgO:Co²⁺ normalized to $H = +10$ kG as a function of temperature: (a) 13°K, (b) 29°K, (c) 51°K. Spectral bandwidth 0.2 nm.

can be both positive and negative within a band (due to either spin-orbit or vibronic effects—see later). f numbers based on these estimates are also given, and emphasize the weakness of the weakest bands detected.

It is also of interest to obtain the minimum Co concentration detectable by MCD. Extrapolating to the saturation limit of ΔA ¹⁶ and taking the instrumental sensitivity at 500 nm to be 2×10^{-6} ,¹⁹ the minimum value of nl , where n is the Co-to-Mg ratio and l is path length in cm, giving an observable MCD is $\sim 10^{-8}$.

Along with the enhanced sensitivity of MCD in detecting transitions goes a greater liability to interference by impurities, particularly paramagnetic impurities. Before entering into a more detailed analysis of the spectrum, therefore, it is necessary to examine the possible involvement in the visible-uv spectra of other first-row transition-metal ions and also of Co²⁺ ions associated with other impurities or defects (including other Co²⁺ ions). In considering other transition-metal ions, we have examined known MgO: M^{n+} absorption spectra and MCD (the latter being limited to Ni²⁺³) and also known $M(\text{H}_2\text{O})_6^{n+}$ absorption and MCD spectra,²⁰⁻²² since there generally exists close similarity in both absorption and MCD between MgO: M^{n+} and $M(\text{H}_2\text{O})_6^{n+}$. Taking into account also approximate concentrations of impurity ions where known from the EPR spectrum, we conclude that contributions from all ions except Mn²⁺ and Fe³⁺ can be definitely excluded. There is some small possibility that Mn²⁺ and/or Fe³⁺ could contribute to the bands at $\lambda < 450$ nm, but this appears very unlikely. At the Co concentration present and assuming a statistical distribution of impurities and lattice defects, the

number of Co²⁺ ions closely associated with another ion or defect is at least two orders of magnitude smaller than the number of essentially cubic ions. In order that the observed bands be primarily due to perturbed Co²⁺ $d-d$ transitions, it is then necessary that the perturbation enhance the intensity by two to three orders of magnitude. A lattice defect would not be expected to cause such major intensification. Marked intensity enhancement has been observed, however, in spin-forbidden transitions of exchange-coupled transition-metal ions, particularly Mn²⁺,²³ and interference from Co²⁺ ions coupled to other Co²⁺ ions or other paramagnetic impurities is a more serious possibility. The most numerous species should be Co²⁺-Co²⁺ pairs. The nearest-neighbor (nn) Co²⁺-Co²⁺ pair has been shown to be antiferromagnetic with an exchange splitting of 26°K.²⁴ MCD C terms can arise only from the

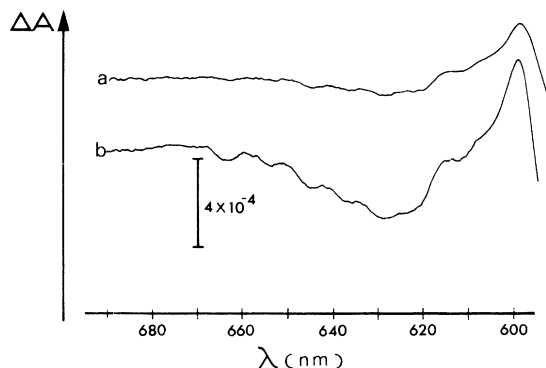


FIG. 6. MCD spectrum of the 16 000-cm⁻¹ band of MgO:Co²⁺ at $H = +40.0$ kG and (a) 33°K, (b) 12°K. Spectral bandwidth 2 nm; period 30 sec.

upper triplet pair state and their intrinsic $1/T$ dependence is hence modulated by a population factor vanishing as $T \rightarrow 0$ K. The T dependence of the main features of the observed MCD¹⁵ is definitely inconsistent with that predicted for the nearest-neighbor pair. (Some weak features may be exceptions—see later). The same argument applies to the next-nearest-neighbor pair, which is even more strongly antiferromagnetic.^{24,25} More distant pairs with smaller—possibly ferromagnetic—exchange interactions could give MCD consistent with the observed T dependence, but the smaller interaction should also reduce the intensity enhancement. It appears, therefore, that Co^{2+} - Co^{2+} pairs are unlikely to be the main source of MCD intensity, and this conclusion should also hold for other possible, less abundant clusters.

Further verification of these conclusions could be obtained by examining the absorption and MCD spectra of crystals containing much higher concentrations of the possible impurity ions, by measuring the Co^{2+} concentration dependence and the T and H dependence at lower temperatures of the MCD, and, most definitively, through EPR-MCD double-resonance experiments.²⁶ We hope to do this in the future; for the remainder of the discussion, however, we assume that essentially all visible-uv bands arise from cubic single Co^{2+} ions.

The absorption intensity of $d-d$ transitions of single Co^{2+} ions can be either allowed magnetic-dipole or vibration-induced electric dipole in nature. The former mechanism leads to a temperature-independent absorption intensity of $\langle A \rangle_0$; the latter gives a temperature-dependent intensity of the form

$$\langle A \rangle_0 = \sum_i \langle A \rangle_{0i}^0 \coth(\hbar\omega_i/2kT) \quad (3)$$

under the simplest approximations, where ω_i is the frequency of the i th vibrational mode.³ Table I shows that the 4T_2 band is predominantly magnetic dipole, $\langle A \rangle_0$ increasing only slightly between 4 and 300 K. On the other hand, the 4T_1 band is seen from Fig. 13 to be predominantly vibration induced, the variation of $\langle A \rangle_0$ with T being very similar to that of the vibration-induced bands of $\text{MgO}:\text{Ni}^{2+}$.³

The intensity mechanism for the other transitions cannot be determined directly in this way since their absorption is too weak. However, ligand-field calculations of the magnetic-dipole intensities permit a reasonably definite conclusion to be reached and confirm the results arrived at for the 4T_2 and 4T_1 bands. With the formula

$$f_{\text{MD}}(A \rightarrow X) = \frac{2m\omega_{XA}}{\hbar e^2} \frac{1}{d_A} \sum_{\gamma, \gamma'} |\langle A_\gamma | \mu_x | X_{\gamma'} \rangle|^2, \quad (4)$$

where $\hbar\omega_{XA}$ is the transition energy, d_A is the degeneracy of A and $\vec{\mu} = -\mu_B(\vec{L} + 2\vec{S})$, and approximating the d orbitals by pure atomic d functions (i.e., assuming the orbital reduction factor to be unity) we calculate the f numbers given in Table I. The agreement with the experimental value for the 4T_2 band is satisfactory, while for the 4T_1 band f_{MD} is two orders of magnitude below that observed, substantiating the T -dependence data. For all other bands, calculated f_{MD} values are appreciably smaller than the experimental values. While the latter are only estimates, they should be lower, rather

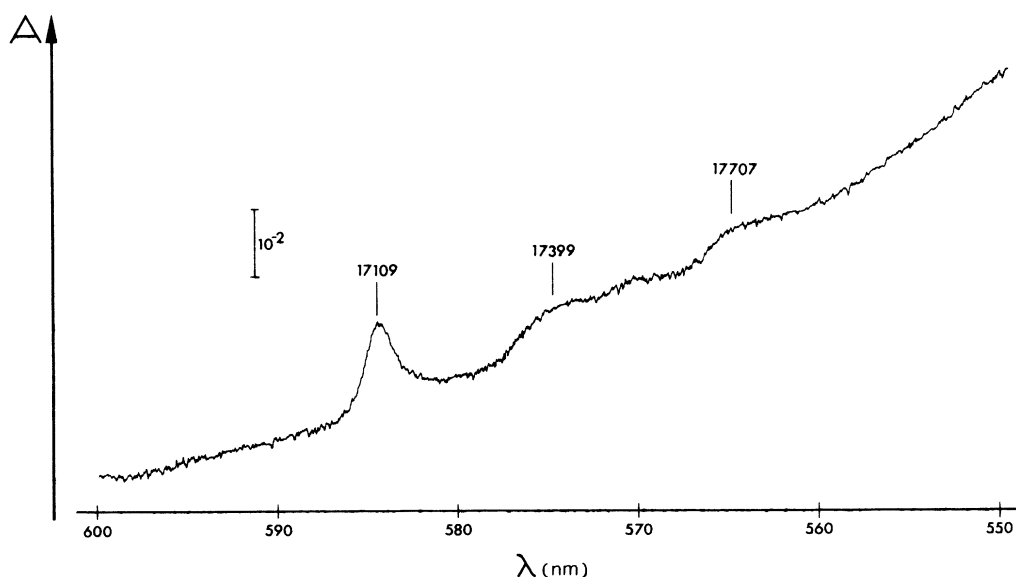


FIG. 7. Absorption spectrum of the 17 000- cm^{-1} band of $\text{MgO}:\text{Co}^{2+}$ at 7°K. Spectral bandwidth ~ 0.25 nm. Energies indicated are in cm^{-1} .

than upper limits to the true values; it is therefore safe to conclude that the intensities of the bands in the visible-uv spectral region are entirely vibration induced.

The ligand-field parameters used for the energy and f_{MD} calculations reported in Fig. 3 and Table I were chosen to best fit the experimental transition energies under two assumptions; first, that all bands except 4T_2 are vibration induced; second, that the $17\,000\text{-cm}^{-1}$ band is due to the 4A_2 , and not 2T_1 and/or 2T_2 , levels. The former assumption was justified above; its consequence is that the average energy of the observed intensity lies above the true vertical electronic transition energy by an amount relating to the vibronic intensity mechanism.³ On this account, in adjusting the ligand-field calculations to the data, the energies of the visible-uv bands were reduced by $\sim 300\text{ cm}^{-1}$. The second assumption is the conventional assignment of the weak band generally observed in octahedral Co^{2+} systems to lower energy of the 4T_1 bands. The

intensity relative to the 4T_1 band is of the order of magnitude expected, assuming the intensity to be proportional to the weight of one-electron excitation and hence $f({}^4A_2):f({}^4T_1) \sim \langle {}^4T_1(t_2^4e^3) | {}^4T_1(G) \rangle^2$, where $\langle {}^4T_1(t_2^4e^3) | {}^4T_1(G) \rangle \sim 0.27$ is the coefficient of the ${}^4T_1(t_2^4e^3)$ function in the ground state. However, it should be noted that, on energy criteria alone, a not unreasonable fit can be obtained by identifying the $16\,000\text{-}$ and $17\,000\text{-cm}^{-1}$ bands with the 2T_1 and 2T_2 levels and including the 4A_2 state in the 4T_1 band (for example, with $\Delta = 9520$, $B = 765$, $C = 3750$, $\zeta = 500\text{ cm}^{-1}$) an assignment suggested by Low.¹⁰ Our data do not lead to a definitive exclusion of this latter assignment.

In earlier work on $\text{MgO}:\text{Ni}^{2+3}$ it was possible to arrive at a detailed understanding of the absorption and MCD intensities and band shapes of the vibration-induced $d-d$ transitions observed. The analysis for $\text{MgO}:\text{Co}^{2+}$ is more complex for two reasons. First, experimentally there is very little resemblance between the MCD of different bands.

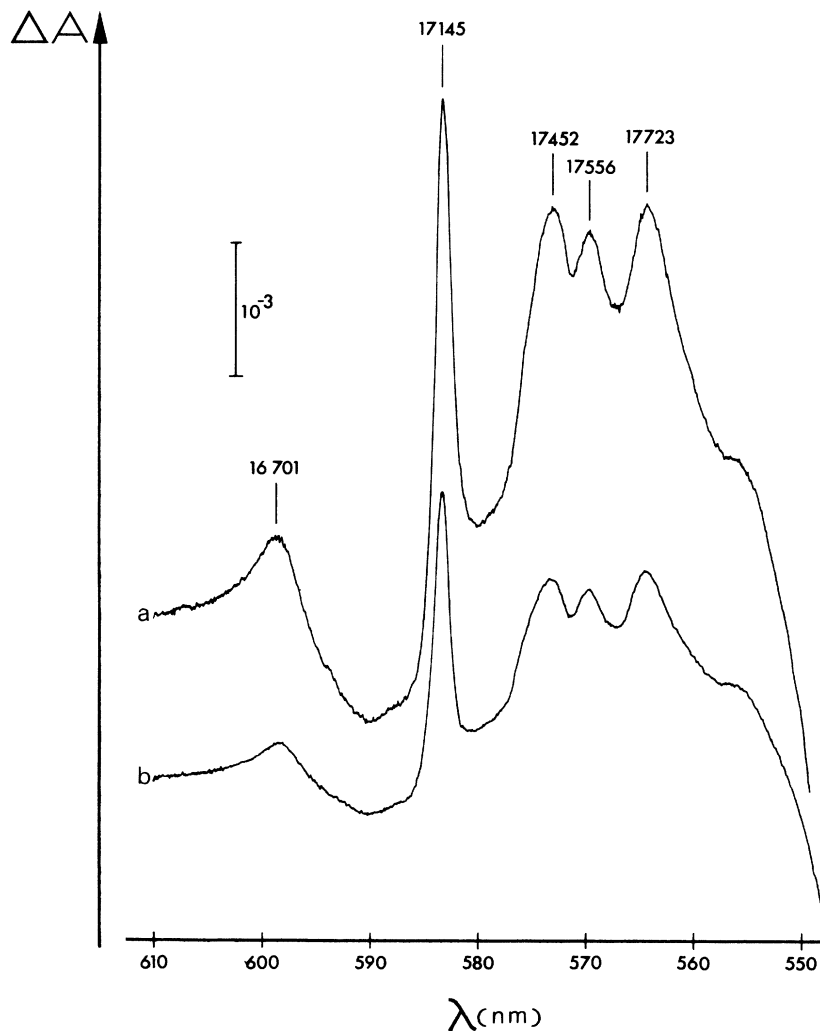


FIG. 8. MCD spectrum of the $17\,000\text{-cm}^{-1}$ band of $\text{MgO}:\text{Co}^{2+}$ at (a) 12°K , $H = +45.1\text{ kG}$ and (b) 33°K , $H = +43.3\text{ kG}$. Spectral bandwidth $\sim 0.13\text{ nm}$; period 30 sec . Energies indicated are in cm^{-1} .

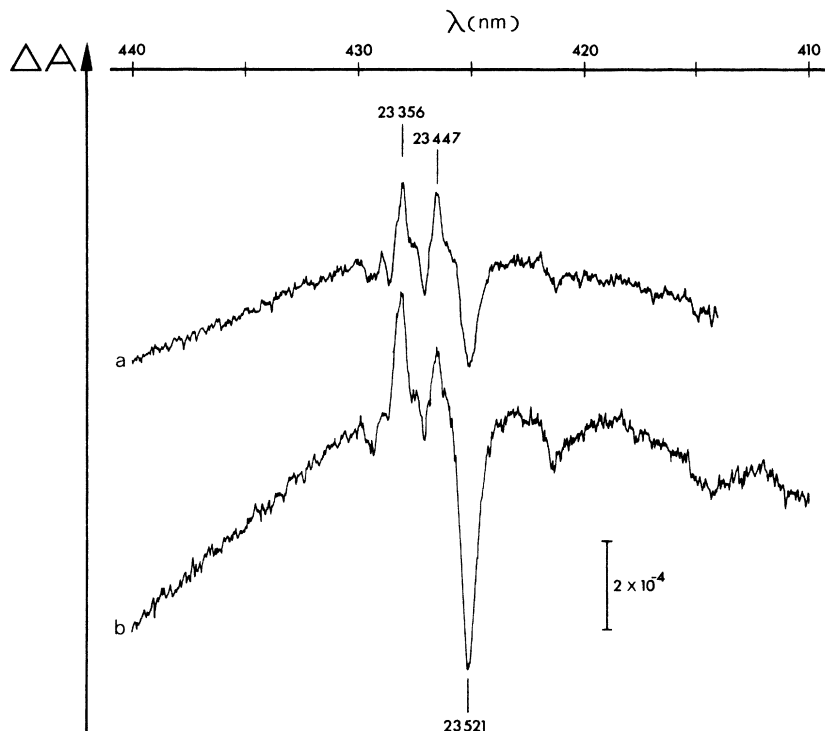


FIG. 9. MCD spectrum of the $23\,000\text{-cm}^{-1}$ band of $\text{MgO}:\text{Co}^{2+}$ at $H = +45.1$ kG and (a) 32°K , (b) 12°K . Spectral bandwidth ~ 0.11 nm; period 30 sec. Energies indicated are in cm^{-1} .

Second, theoretical calculations are more difficult and less symmetry determined. At present we do not have a complete quantitative interpretation of the data, and the following discussion is qualitative in nature.

We first discuss the bands exhibiting appreciable fine structure, excluding the 4T_1 band and the bands at $\lambda > 585$ nm. Since all the bands are vibronic, one-phonon excitations in u modes must occur. The calculations of Sangster and McCombie^{27,28} and Manson²⁹ (SMM) show that these lie principally between 200 and 600 cm^{-1} above the zero-phonon energy. Comparison with the observed bands shows that the energy spread of the principal features nowhere much exceeds 400 cm^{-1} if the possible spin-orbit splitting of the $25\,000\text{-cm}^{-1}$ 2T_2 band is allowed for. These can therefore be attributed principally to one-phonon sidebands. Multiphonon excitations are probably present to some extent but are much weaker in intensity, indicating that the excited states differ little in geometry from the ground state.

In the simplest possible situation in which the transition moment couples to only one nearest-neighbor nuclear displacement symmetry coordinate, the dispersion of the band of one-phonon excitations is provided by the SMM calculations. It is easy to show that, in addition, the C term of the MCD is of one sign and has the same dispersion. Conversely, C terms of varying sign are a definite indication of coupling to multiple vibrational coor-

dinates.

The 2A_1 state is susceptible to neither spin-orbit splitting nor Jahn-Teller effects and would be expected to exhibit a simple band structure. The observed complexity (Fig. 9) can only result from vibronic coupling involving more than one nuclear

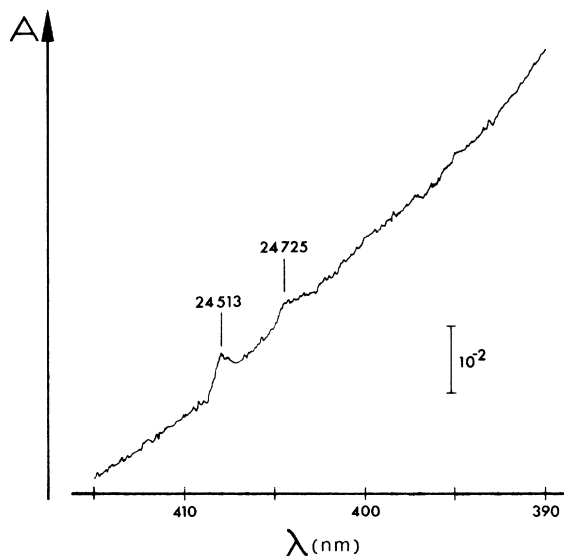


FIG. 10. Absorption spectrum of the $25\,000\text{-cm}^{-1}$ band of $\text{MgO}:\text{Co}^{2+}$ at 7°K . Spectral bandwidth ~ 0.36 nm. Energies indicated are in cm^{-1} .

coordinate. The 23447-cm^{-1} feature is noticeably less T dependent than the remainder of the band and is either an A term¹⁴ (arising from Zeeman splittings) or due to another species (e.g., antiferromagnetic $\text{Co}^{2+}\text{-Co}^{2+}$ pair). Even if the latter obtains, however, the earlier conclusion is not affected.

The 25000-cm^{-1} 2T_2 band (Figs. 10 and 11) provides the only structure clearly resembling a predicted dispersion, specifically that for coupling to the $t_{1u}^{(1)}$ (stretching) MO_6 coordinate.^{27,29} The principal peaks lie 221 cm^{-1} apart, the order of magnitude expected. However, this splitting also coincides very closely with the predicted spin-orbit splitting of 234 cm^{-1} and an alternative assignment of the two peaks is to phonon sidebands of the same energy of the E'' and U' states. In the first assignment, if the main features are due to E'' , the 25044-cm^{-1} extremum could be associated with the U' state, either with sidebands beginning at much higher energy than E'' , or with lower-energy sidebands hidden beneath the 24764-cm^{-1} peak. Alternatively the main features are due to U' ; this requires the E'' band to be too weak to be visible and a more complex vibronic coupling to explain the

sideband structure, seeming less likely. The second assignment makes the interpretation of the high-energy structure difficult. Altogether, we prefer the assignment of the 24543- , 24764- , and 25044-cm^{-1} extrema to E'' , $E'' + U'$, and U' sidebands, respectively.

The 27000-cm^{-1} 2T_1 band (Fig. 12) shows no obvious sign of the predicted spin-orbit splitting of 79 cm^{-1} and is too weak to make interpretation feasible.

The 28000-cm^{-1} 2E band (Fig. 12) shows complicated structure. While this state is in principle subject to Jahn-Teller effects, any appreciable interaction would lead to a much broader band than is observed and this can be excluded. The 27933- and 28129-cm^{-1} features are not very T dependent and might arise from other species than single Co^{2+} ions. Even if that were the case, however, the band structure requires interaction with multiple vibrational coordinates.

The 17000-cm^{-1} 4A_2 band (Figs. 7 and 8) also bears no resemblance to any of the SMM calculations, despite being predominantly of one sign.

Of the five highly structured bands, therefore, only one shows vibrational structure having the pos-

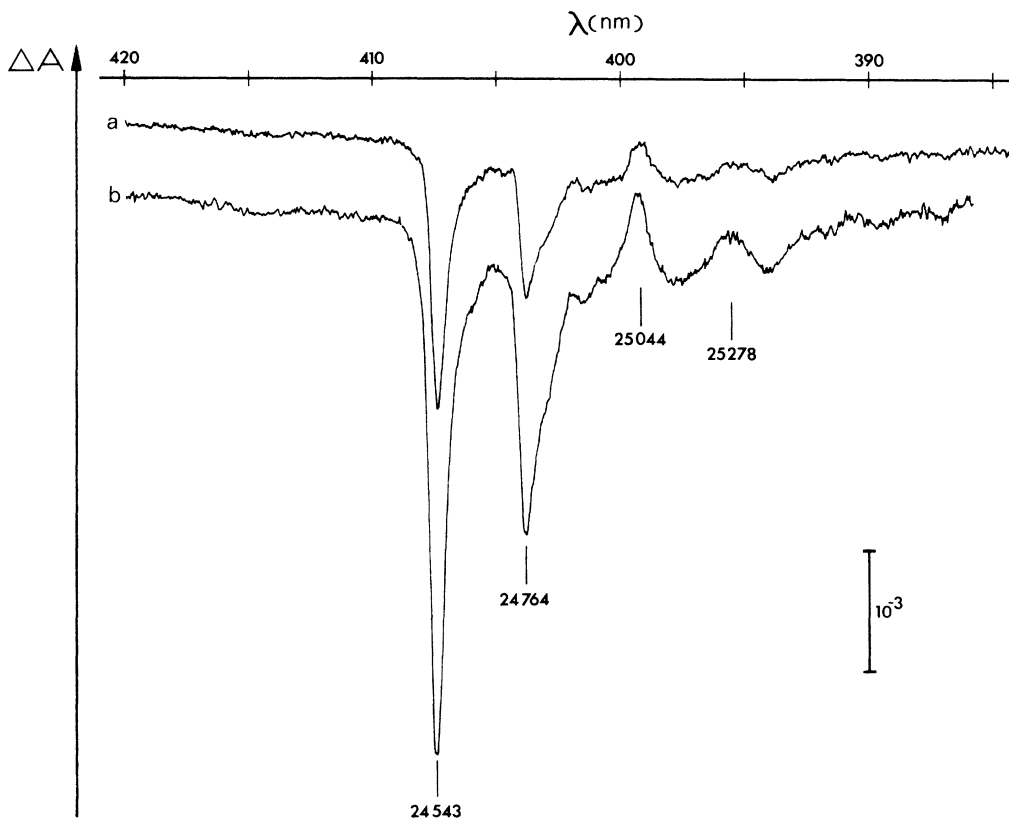


FIG. 11. MCD spectrum of the 25000-cm^{-1} band of $\text{MgO}:\text{Co}^{2+}$ at (a) 32°K , $+45.1\text{ kG}$ and (b) 15°K , $+45.6\text{ kG}$. Spectral bandwidth $\sim 0.044\text{ nm}$; period 30 sec . Energies indicated are in cm^{-1} .

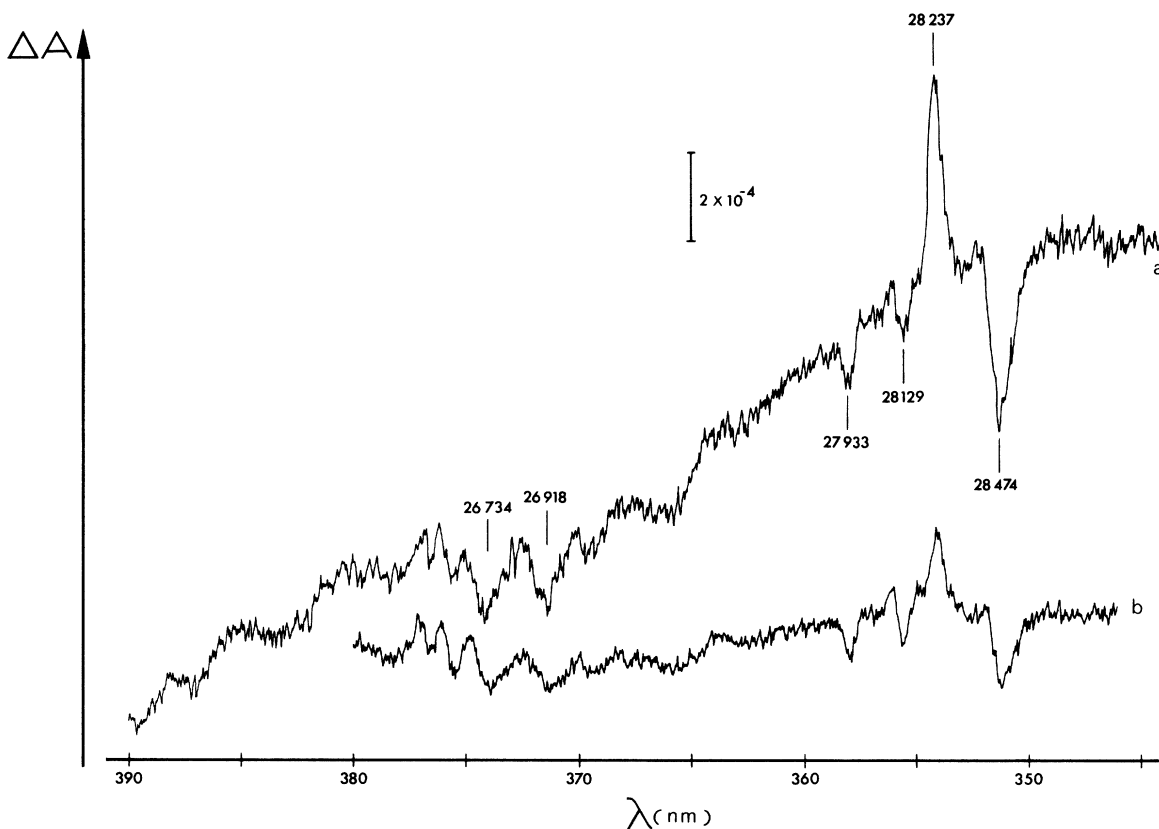


FIG. 12. MCD spectrum of the 27 000- and 28 000- cm^{-1} bands of $\text{MgO}:\text{Co}^{2+}$ at $H=+45.1$ kG and (a) 12°K, (b) 33°K. Spectral bandwidth 0.2 nm; period 30 sec. Energies indicated are in cm^{-1} .

sibility of a simple interpretation in terms of the SMM calculations. This contrasts totally with the phonon-assisted bands of $\text{MgO}:\text{Ni}^{2+}$, which all show very similar structure closely corresponding to the SMM $t_{1u}^{(1)}$ coupling calculations.^{3,29,30} Further, the only other structured, phonon-assisted bands clearly observed in $\text{MgO}:M^{n+}$ systems, namely, the ${}^2E \rightarrow {}^4A_2$ emission bands of V^{2+} and Cr^{3+} have been satisfactorily fit assuming essentially pure $t_{1u}^{(1)}$ and t_{2u} coupling, respectively.^{27,28} More work is clearly required to establish whether SMM-type calculations can explain the observed Co^{2+} band shapes, or whether it is necessary to invoke coupling to displacements of ions beyond nearest neighbors.

The bands to lower energy than the 17 145- cm^{-1} peak are both broad and peculiar and do not suggest obvious detailed analysis. There remains the 4T_1 band. The 4T_1 and neighboring 2T_1 levels are strongly mixed by spin-orbit coupling and the final states span nearly 2000 cm^{-1} . The simplest interpretation of the band attributes the width and shape to phonon sidebands superimposed on this broad electronic manifold. Insufficient structure is re-

solved to enable detailed confirmation of this picture. An alternative, more complex possibility involves attributing the gross three-pronged structure of the absorption spectrum to a Jahn-Teller interaction between the 4T_1 state and t_{2g} vibrations. Such a band shape is predicted theoretically in this case³¹ and various experimental observations have been interpreted in terms of this model.³² A prediction of this model is that at high temperatures the outer peaks will diverge from the central peak approximately proportionately to \sqrt{T} . Absorption measurements up to 469°K (Fig. 4) show no dependence of this form within experimental error and offer no support to the postulate of a Jahn-Teller effect in the band.

In principle, the sign and magnitude of the MCD of a vibration-induced transition depends on the excited electronic state, the nature of the active vibration and the details of the vibronic mechanism.³ For $\text{MgO}:\text{Ni}^{2+}$ it was possible to establish from the MCD that the observed intensity was induced essentially entirely via t_{1u} phonons.³ Unfortunately, for $\text{MgO}:\text{Co}^{2+}$ the theoretical calculations are very much more complex, owing principally to the or-

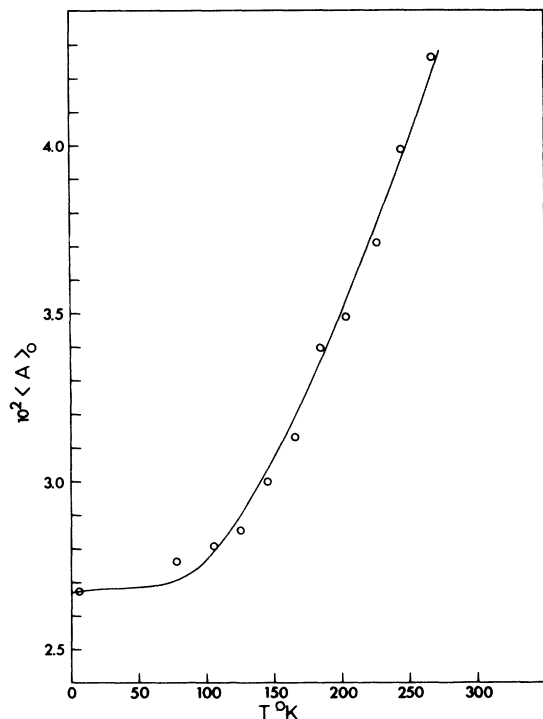


FIG. 13. Temperature dependence of the absorption zeroth moment, $\langle A \rangle_0$, of the 20 000-cm⁻¹ band. Full line represents the equation $\langle A \rangle_0 = \langle A \rangle_0^0 \coth(\hbar\omega/2kT)$ with $\langle A \rangle_0^0 = 2.67 \times 10^{-2}$, $\hbar\omega = 279$ cm⁻¹.

bital degeneracy of the ground state and the results, unlike for MgO: Ni²⁺, are not in general group-theoretically determined. Such calculations, under various approximations, have been reported for octahedral Co²⁺ by Harding and Briat in their MCD study of Co(H₂O)₆(BrO₃)₂.²² However, the combined uncertainties in the theory and in our band-shape analysis inhibit arrival at any definite conclusions from the calculations. The ⁴A₂ band constitutes an exception to this situation. Ignoring second-order spin-orbit coupling, group theory alone predicts positive and negative MCD C terms for coupling to *t*_{1u} and *t*_{2u} vibrations, respectively. Our assignment of the 17 000-cm⁻¹ band then requires its intensity to be generated predominantly through *t*_{1u} phonons.

It is of interest to compare our MCD data and analysis for MgO: Co²⁺ with those of Harding and Briat (HB) for Co(H₂O)₆(BrO₃)₂.²² The near equality in ligand field strength of O²⁻ and H₂O is expected to lead to similarities in the energy levels. On the other hand, the differences in site symmetry and vibrational spectrum can lead to dissimilar band shapes. The HB data have much the same over-all character as ours: the ⁴A₂ and ⁴T₁ bands give broad positive and negative MCD bands, respec-

tively (the latter spreading to higher energy than in MgO: Co²⁺ due to sidebands in the high-frequency H₂O vibrations); above the ⁴T₁ band a number of weak bands are observed. However, the detailed structures of the latter bear no resemblance to the MgO: Co²⁺ data, with the exception of the 26 000-cm⁻¹ band which quite strikingly resembles our 25 000-cm⁻¹ band. This would be satisfactory if the HB assignment of their band were ²T₂. However, in fact HB assign their band to ²T₁ and their assignment of the spin-forbidden transitions is altogether out of phase with ours. We suggest tentatively that our assignment is correct and that the HB assignment is incorrect and should be instead ²A₁, 25 000 cm⁻¹; ²T₂, 26 000 cm⁻¹; ²T₁, 27 000 cm⁻¹; ²E, 29 000 cm⁻¹, on the grounds that (i) except for the ²T₁ level within the ⁴T₁ band, all doublet states are observed clearly in MgO, whereas in Co(H₂O)₆(BrO₃)₂ the greater breadth of the ⁴T₁ band obscures the 23 000–25 000-cm⁻¹ region; (ii) the correlation of calculated and observed energies is much better for our assignments than for the HB interpretation; (iii) the MCD of the Co(H₂O)₆²⁺ 26 000-cm⁻¹ band indicates assignment to ²T₂ by comparison with MgO: Co²⁺. These arguments are not definitive and further evidence to resolve this disagreement is required. It is possible that a detailed analysis of

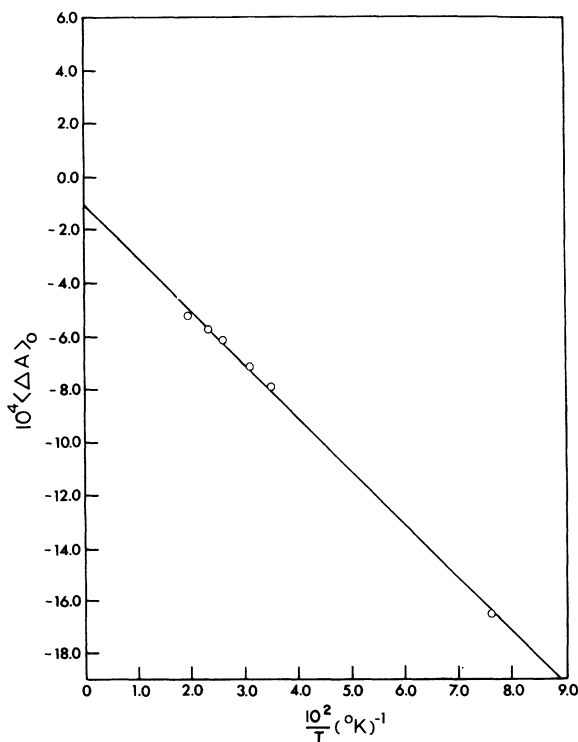


FIG. 14. Temperature dependence of the MCD zeroth moment, $\langle \Delta A \rangle_0$, of the 20 000-cm⁻¹ band. MCD is normalized to +10 kG.

TABLE I. Experimental and calculated spectral parameters.

State	Calculated energy ^a (cm ⁻¹)	Band energy ^b (cm ⁻¹)	$\langle A \rangle_0$	f^c	$f_{MD}^{a,d}$	
4T_1	E'	0				
	U'	329				
	U''	859				
	E''	951				
4T_2	E'	8353	9000	$1.1 \times 10^{-2} e, f$	7.1×10^{-6}	
	U'	8385				
	U''	8475				
	E''	8678				
2E	U'	8926				
2T_1	U'	15812	16000 ^g	$1 \times 10^{-4} h$	1×10^{-7}	
	E'	16296				
2T_2	U'	16514				
	E''	16747				
4A_2	U'	17461	17000 ⁱ	$\begin{cases} 2.0 \times 10^{-4} e \\ (2 \times 10^{-4})^h \end{cases}$	$\begin{cases} 2.5 \times 10^{-7} \\ (2 \times 10^{-7}) \end{cases}$	4.5×10^{-11}
4T_1	U'	19030	20000	$2.7 \times 10^{-2} e$	3.9×10^{-5}	
	E''	19164				
	U''	19169				
	E'	19558				
2T_1	U'	20730				
	E'	20813				
2A_1	E'	23011	23000	$8 \times 10^{-6} h$	1×10^{-8}	3.9×10^{-10}
2T_2	E''	24696	25000	$1 \times 10^{-4} h$	2×10^{-7}	
	U''	24930				
2T_1	U'	25958	27000	$3 \times 10^{-6} h$	5×10^{-9}	
	E'	26037				
2E	U'	27869	28000	$7 \times 10^{-6} h$	1×10^{-8}	0.7×10^{-10}

^aFor $\Delta=8950$, $B=800$, $C=3750$, $\zeta=500$ (all in cm⁻¹).

^bApproximate location.

^cFrom $\langle A \rangle_0$, using Eq. (2).

^dCalculated (see text).

^eFrom 7°K absorption spectrum.

^f $\langle A \rangle_0 = 1.3 \times 10^{-2}$ at 254°K.

^g $\lambda > 585$ nm.

^hEstimated from MCD (see text).

ⁱ $\lambda = 585-557.5$ nm in MCD.

the natural CD of $\text{Co}(\text{H}_2\text{O})_6^{2+}$, observed in $\alpha\text{-Zn}(\text{H}_2\text{O})_6\text{SeO}_4:\text{Co}^{3+}$ will provide such evidence.

IV. CONCLUSION

Our work has located several new excited states of Co^{2+} in MgO, and exhibited the great sensitivity of MCD, both in observing weak transitions and in detecting the presence of impurity ions. For example, MCD should permit the spectra of other ions in MgO to be much better characterized, particularly Mn^{2+} and Fe^{3+} whose $d-d$ transitions are entirely limited to spin-forbidden transitions and most of which are currently unknown. MCD should also allow detection of optical transitions of ions produced in low concentration by irradiation, chemical treatment, and so on. Fe^+ , isoelectronic with Co^{2+} and generated in MgO by uv and x irradiation from Fe^{2+} ,³⁴ is an obvious candidate. A further

bonus of the sensitivity of MCD is that it allows weak transitions of single impurity ions to be studied at concentrations low enough to avoid complications from ion aggregation.

Most of the new states observed in $\text{MgO}:\text{Co}^{2+}$ exhibit considerable fine structure and greatly increase the number of structured vibration-induced bands known for impurity transition-metal ions in MgO. Quantitative band-shape calculations have recently been carried out for phonon-assisted transitions of V^{2+} , Cr^{3+} , and Ni^{2+} in MgO with reasonable success.²⁷⁻³⁰ However, we have been able to interpret very few of the observed structures in $\text{MgO}:\text{Co}^{2+}$ in terms of these calculations. Our data thus require refinement of current band-shape theory for impurities in MgO. Further calculations are also required to identify the routes by which the $d-d$ transitions gain intensity.

Further experiments to substantiate our assign-

ment of the MCD spectrum to specific excited states of single Co^{2+} ions are indicated and such work is being undertaken. We are also investigating the MCD and stress-induced linear dichroism of the infrared spectral bands.^{4,5}

The effects of exchange interactions on optical spectra is a topic of considerable interest currently. Our work should form a useful basis for further investigations of the spectra of Co^{2+} ion clusters in MgO and of the antiferromagnetic CoO .

ACKNOWLEDGMENTS

We gratefully acknowledge the generous assistance of Cary Instruments and especially of Dr.

J. J. Duffield and Dr. A. Abu-Shumays in MCD experiments at Cary Instruments; the gift of $\text{MgO}:\text{Co}$ crystals by Dr. B. Henderson; the use of a Dewar by Professor D. A. Dows; the use of a least-squares fitting program by Dr. P. K. Rawlings; the measurement of EPR spectra by Professor J. Hurrell; a preprint of Ref. 22 from Dr. B. Briat; advice and assistance from Dr. G. A. Osborne and Dr. B. D. Bird; an Alfred P. Sloan Foundation Fellowship (to P. J. S.) a National Science Foundation Trainee Research Fellowship and a Stauffer Chemical Company Fellowship (to A. J. M.) and grants from the National Institutes of Health and the National Science Foundation.

*Alfred P. Sloan Research Fellow.

¹See, for example C. J. Ballhausen, *Introduction to Ligand Field Theory* (McGraw-Hill, New York, 1962); J. Ferguson, *Prog. Inorg. Chem.*, **12**, 159 (1970).

²For recent reviews, see C. H. Henry and C. P. Slichter, *Physics of Color Centers*, edited by W. B. Fowler (Academic, New York, 1968), p. 351; P. N. Schatz and A. J. McCaffery, *Q. Rev. Chem. Soc.* **23**, 552 (1969).

³B. D. Bird, G. A. Osborne, and P. J. Stephens, *Phys. Rev. B* **5**, 1800 (1972).

⁴G. A. Osborne, J. C. Cheng, and P. J. Stephens, *Rev. Sci. Instrum.* **44**, 10 (1973).

⁵J. C. Cheng, A. Mann, G. A. Osborne, and P. J. Stephens, *J. Chem. Phys.* **57**, 4051 (1972).

⁶G. A. Osborne and P. J. Stephens, *J. Chem. Phys.* **56**, 609 (1972).

⁷2724 S. Peck Rd., Monrovia, Calif., 91016.

⁸R. Pappalardo, D. L. Wood, and R. C. Linares, *J. Chem. Phys.* **35**, 2041 (1961).

⁹J. E. Ralph and M. G. Townsend, *J. Chem. Phys.* **48**, 149 (1968).

¹⁰W. Low, *Phys. Rev.* **109**, 256 (1958).

¹¹Dr. D. L. Wood estimates the accuracy of the concentration given in Ref. 6 as ± 10 – 20% (private communication).

¹²Ligand-field calculations have been carried out with two different programs: a strong-field program, written by Dr. B. D. Bird and a weak-field program, using the matrices in J. Ferguson, *Aust. J. Chem.* **23**, 635 (1970). The programs give energies in agreement with previously reported calculations (e.g., J. Ferguson, D. L. Wood, and K. Knox, *J. Chem. Phys.* **39**, 881 (1963)).

¹³The unobserved states above $28\,000\text{ cm}^{-1}$ predicted by ligand-field theory are not included.

¹⁴P. J. Stephens, *J. Chem. Phys.* **52**, 3489 (1970).

¹⁵More precisely, ignoring band-shape changes, the MCD C terms should vary as $\tanh(g\mu_B H/2kT)$. At low H and/or high T this equals $g\mu_B H/2kT$; at our lowest T (12°K) and highest H (46 kG) $\tanh(g\mu_B H/2kT) = 0.91(g\mu_B H/2kT)$. The 4T_1 band MCD varies accurately as H/T at H/T values small enough to keep the MCD from exceeding the least sensitive scale of the Cary 61. The other bands

follow $\tanh(g\mu_B H/2kT)$ within experimental error.

Note, however, that the maximum degree of saturation obtained is not sufficient to enable g to be reliably determined experimentally.

¹⁶Extrapolated from lower fields assuming ΔA varies as $\tanh(g\mu_B H/2kT)$.

¹⁷Average sensitivity estimated from Cary 61 manual assuming zero absorbance, 2nm spectral bandwidth and 30 sec period.

¹⁸This procedure works satisfactorily for the $17\,000\text{ cm}^{-1}$ band, whose $\langle A \rangle_0$ can be measured directly, as shown in Table I.

¹⁹Estimated as in Ref. 17.

²⁰A. J. McCaffery, P. J. Stephens, and P. N. Schatz, *Inorg. Chem.* **6**, 1614 (1967).

²¹M. J. Harding, S. F. Mason, D. J. Robbins, and A. J. Thomson, *J. Chem. Soc. A* 3047 (1971).

²²M. J. Harding and B. Briat, *Mol. Phys.* **25**, 745 (1973).

²³See, for example, L. L. Lohr and D. S. McClure, *J. Chem. Phys.* **49**, 3516 (1968).

²⁴S. R. P. Smith, Ph.D. thesis (Oxford University, 1966) (unpublished).

²⁵J. Kanamori, *Prog. Theor. Phys.* **17**, 177 (1957).

²⁶Such experiments have been carried out on the charge-transfer bands of $\text{MgO}:\text{Fe}^{3+}$ by J. C. Cheng, and J. C. Kemp, *Phys. Rev. B* **4**, 2841 (1971).

²⁷M. J. L. Sangster and C. W. McCombie, *J. Phys. C* **3**, 1498 (1970).

²⁸M. J. L. Sangster, *Phys. Rev. B* **6**, 254 (1972).

²⁹N. B. Manson, *Phys. Rev. B* **4**, 2645 (1971); *Phys. Rev. B* **4**, 2656 (1971).

³⁰Note that the interpretation of the infrared 3T_2 emission of $\text{MgO}:\text{Ni}^{2+}$ in Refs. 27 and 29 is incorrect, since the transition mechanism is in fact magnetic dipole (Ref. 3).

³¹E. Englman, *The Jahn-Teller Effect in Molecules and Crystals*, (Wiley, New York, 1972), Chap. 3.

³²W. Ulrici, *Phys. Status Solidi B* **44**, K29 (1971).

³³K. D. Gailey and R. A. Plamer, *Chem. Phys. Lett.* **13**, 176 (1972).

³⁴J. W. Orton, P. Auzins, J. H. E. Griffiths, and J. E. Wertz, *Proc. Phys. Soc. (Lond.)* **78**, 554 (1961).